On Nanocomposite Fabrication: Using Rheology to Characterize Filler/Polymer Interactions in Epoxy Based Nanocomposites

Fuad N. Alhabill[a,*], *Alun S. Vaughan*[b], *Thomas Andritsch*[b]

[a] Electronics & Electrical Engineering, Department of Engineering and Design, University of Chichester, Chichester PO19 6PE, United Kingdom

[b] Tony Davies High Voltage Laboratory, Electrical Power Engineering Group, University of Southampton, Southampton SO17 1BJ, United Kingdom

[*] Corresponding author: Fuad N. Alhabill, E-mail: f.alhabill@chi.ac.uk

HIGHLIGHTS:

- Rheological characterization has been used to detect filler/polymer interactions during nanocomposite preparation.
- These interactions can be exploited to provide an innovative experimental approach to nanocomposite fabrication.
- Such approach could be engineered to optimize filler/matrix interactions, enhance particle dispersion and introduce required functional groups into the final system.
- The study highlights the critical impact of material processing on macroscopic properties of resulting nanocomposites.

ABSTRACT:

The interactions that occur between an amorphous silicon nitride (Si_3N_4) nanofiller and an epoxy matrix are examined, as revealed by rheological changes in a diglycidyl ether of bisphenol-A

(DGEBA)-based epoxy resin prior to curing and thermal analysis, scanning electron microscopy and dielectric spectroscopy of the resulting amine-cured systems. The results show that isothermally heating the as-received Si_3N_4 in DGEBA at 100 °C leads to increases in the viscosity of the mixture. Analysis of rheological data obtained from unfilled, as-received Si_3N_4-filled and calcined Si_3N_4-filled epoxy systems leads us to interpret this increase in viscosity as arising from reactions between epoxide groups of the DGEBA and nanoparticle surface groups, notably involving surface amines, which are stimulated by the elevated temperature. The extent of this filler/resin reaction depends on the material processing protocol used, particularly prior calcination of the Si_3N_4 and the temperature and duration of nanoparticle/DGEBA mixing. Glass transition temperature data show that cured samples prepared using different methods have significantly different glass transition temperatures, which is a consequence of the epoxide/amine stoichiometric imbalances that result from prior reactions between the Si_3N_4 and the DGEBA. Consistent behavior was observed in the dielectric response. These results demonstrate that ultimate macroscopic properties of Si_3N_4/epoxy nanocomposites are critically affected by details of the processing protocol. Furthermore, we infer that, by using controlled prior calcination of the Si_3N_4, it is may be possible to vary the initial surface chemistry of the nanoparticles so as to adjust their reactivity with epoxy-containing moieties. Here, this is exemplified using only two somewhat extreme thermal treatments and a bifunctional DGEBA-type compound but, we suggest, that the concept may be extended to many other mono- and polyfunctional epoxy-containing compounds in order to generate a wide range of different grafted nanoparticle systems. This strategy may provide a versatile means of adjusting the surface chemistry of inorganic nitride nanoparticles, in order to tailor their surface chemistry and thereby modify resulting nanocomposite properties.

KEYWORDS: Polymer nanocomposites, interface, filler/polymer interactions, rheology, material processing, particle dispersion, glass transition

1. INTRODUCTION

Nanocomposites have captured a burgeoning research interest over recent decades as a means of improving, as required, the electrical, mechanical and/or thermal properties of polymers. Nanofillers have an extremely large surface area and the consequent interfacial interactions between the nanofiller surface and the surrounding matrix are often considered to be a critical factor in determining the ultimate properties of the final system [1-5]. However, the fabrication of nanocomposites can be a

challenge in that, due to their extremely large specific surface area and the resulting surface energy, nanoparticles tend to agglomerate within many polymer matrices [2,6,7]. Such agglomerations are considered to be a source of defects that can degrade the properties of the produced nanocomposite [2,8,9] and, as such, a common strategy to improve particle dispersion involves chemically treating the surface in order to add appropriate functionalities [10,11]. This approach is designed to improve the interactions between the nanoparticles and the surrounding polymer and consequently improve the nanoparticle dispersion [2,6]. Depending on the characteristics of the matrix and the nanofiller, these interactions could be chemical [12,13], physical [14] or electrical [15,16] in nature and have often been suggested to result in the formation of interphase regions with modified properties around nanoparticles [5,17,18].

While the extent and nature of such interactions will be affected by the chemistry of the polymer and the surface chemistry of the particles, they may also be affected by the imposed processing protocol used during nanocomposite preparation: *e.g.* the mixing procedure, its duration and the imposed temperature [19,20]. For example, different preparation methods may lead to different particle dispersions and thus different specific particle/polymer interfacial areas [21,22]. Furthermore, using a higher temperature during nanocomposite preparation could stimulate or accelerate potential chemical reactions between particle surface functionalities and active chemical groups within the polymer matrix. This may be more prevalent in thermosetting-based nanocomposite, where particles are introduced into the host matrix before curing. As such, using only slightly different preparation procedure may significantly affect the properties of the resulting nanocomposite, which might explain the discrepancies between results reported in the literature, where different research groups report inconsistent behavior for what, at first glance, appear equivalent polymer-filler-combinations [23,24]. Therefore, investigating the impact of the nanocomposite fabrication method would be beneficial for analyzing the behavior of these systems.

Despite the perceived importance of filler/matrix interactions on the structure and consequent properties of polymeric nanocomposites, the characterization of such local effects is far from trivial [25]. Indeed, many studies have attempted to probe the impact of these interactions by investigating the final nanocomposite system *after* completion of the preparation process, using techniques such as differential scanning calorimetry, dielectric spectroscopy and electron microscopy [4,17,26,27]. Studying the influence of added nanoparticles on the rheological characteristics of a liquid polymer

matrix *during* processing might provide additional complementary information about the interactions occurring between the nanofiller and the polymer. However, few studies have used rheology as a tool for analyzing the dispersion of particles within a polymer [28-30] and, to our knowledge, rheology has not thus far been explored to investigate the presence of nanofiller/matrix interactions and, consequently, to engineer the preparation method of polymeric nanocomposites.

In this study, we set out to investigate interactions between silicon nitride (Si_3N_4) nanoparticles and an epoxy resin matrix, prior to curing. The choice of system was based on the surface chemistry of Si_3N_4 and the hypothesis that this could be stimulated to react with epoxide groups present within the surrounding liquid epoxy resin and that this would manifest itself rheologically. Therefore, the investigation started by observing the rheological properties of the filler/resin mixture as a tool to study and detect any possible interactions. The impact of changing the mixing temperature or duration was explored. Based on the rheological results, selected samples were then cured and prepared for further testing in order to analyze the impact of any possible interfacial interactions on the macroscopic properties of the produced nanocomposite samples. The post-curing characterization considered the dispersion of the nanoparticles within the matrix, changes in the glass transition temperature and variations in the dielectric spectra.

2. MATERIALS AND METHODS

2.1. Materials

A model epoxy resin closely based on diglycidyl ether of bisphenol-A (DGEBA) was chosen for the polymeric matrix. Specifically, DER 332 from Sigma Aldrich was used (epoxide equivalent molar mass of 174 g/mol) and was cured using the polyetheramine hardener, Jeffamine D230 from Huntsman. Based on the epoxide and amine equivalent molar masses, the ideal stoichiometric resin : hardener ratio is 100 : 34.4 parts by weight and this ratio was, therefore, used throughout this study. Amorphous silicon nitride (Si_3N_4) nanopowder was used as the nanofiller. According to the supplier (Sigma Aldrich), the particle size of this nanofiller is < 50 nm and particles are close to spherical in shape. The surface chemistry of these nanoparticles is characterized, primarily, by amine and hydroxyl groups [31-33]. In addition to using the nanofiller, as-supplied, an additional nanoparticle system was prepared by calcination of the as-received Si_3N_4 nanopowder at 1050 °C for 10 h. Such a heat

treatment has been demonstrated to remove surface amine and hydroxyl groups to leave a thin layer of silica that is terminated with siloxane bridges [32-34].

The samples investigated in this study can be grouped into three sets: unfilled epoxy; epoxy containing 5 wt% of as-received silicon nitride; epoxy containing 5 wt% of calcined silicon nitride. To prepare a nanocomposite sample, the required nanofiller was first manually mixed with the DGEBA, then exposed to a probe sonicator for 45 min to disperse the particles further. Next, the particle/DGEBA mixture was isothermally heated at a chosen temperature (100 °C here) for a specific period of time, with the aim of stimulating/accelerating chemical reactions between the DGEBA and relevant chemical groups on the surface of the particles (*i.e.* amine and, to a lesser extent, hydroxyl groups). By varying the duration of the isothermal heating step, different samples were produced within each sample set. Following the heating step, the rheological characteristics of the resulting system were determined. Finally, the hardener was added and mixed with the resin for 15 min at room temperature, using a magnetic stirrer. Subsequently, the mixture was degassed at 35 °C for 20 min, before being cast into a steel mold for curing. Curing was performed in a fan oven for 2 h at 80 °C followed by 3 h of post-curing at 125 °C, based on the manufacturer's instructions. The same processing procedure was followed for the unfilled epoxy samples, but with the nanoparticle addition and dispersion steps omitted. All the resulting cured samples were stored under vacuum at room temperature until required (minimum two weeks), to eliminate the possible impact of any absorbed water [35].

For convenience each sample will subsequently be represented using the following designation *LP*/*T*/*t*. In this, *L* represents the nanofiller loading level (0 or 5 wt%), *P* represents the chosen nanofiller processing treatment (U ≡ untreated; C ≡ calcined at 1050 °C), *T* represents the isothermal heating temperature (*i.e.* 100 °C) and *t* represents the total integrated heating time, in hours. Thus, for example, 5U/100/2 refers to a sample filled with 5 wt% of as-received Si_3N_4 and where the filler/resin mixture had been heated at 100 °C for 2 h before rheological characterization.

2.2. Rheological Characterization

Rheological characterization was conducted using a Paar Physica Rheolab MC1 concentric cylinder rheometer, which was located within a temperature-controlled water bath. For each specimen,

the shear stress was linearly increased from 1 to 60 Pa and, at each point, the shear rate was measured. The Physica Rheologic RS 100 software package was used for instrument control and data collection.

2.3. Characterization of Cured Systems

The effect of material processing on the properties of the cured samples was investigated by examining the glass transition temperature, the dielectric spectra and the particle dispersion.

The glass transition temperature (T_g) of the cured samples was measured using a Perkin Elmer DSC7 differential scanning calorimeter (DSC). This was routinely calibrated using high purity indium and, then, the specimen of interest (~10 mg in mass) was subject to two consecutive DSC scans from 50 °C to 150 °C at a heating rate of 10 °C/min. The first scan was used to erase the thermal history of the specimen and T_g was evaluated from the second scan. T_g was considered to correspond to the temperature corresponding to the maximum gradient in the heat capacity curve. For each system, these measurements were repeated three times using different specimens, to evaluate the uncertainty in the obtained data.

Dielectric spectra of the cured samples were acquired using a Solartron 1296 dielectric interface along with a Schlumberger SI 1260 impedance/phase gain analyzer and a measurement cell with two circular parallel plates 30 mm diameter. Specimens, 200 ± 10 μm in thickness, were sputtered-coated on both side with gold to improve the contact between the sample and the cell's electrodes. All measurements were conducted at room temperature.

Nanoparticle dispersion within the epoxy matrix was examined using a JEOL JSM-6500F scanning electron microscope (SEM) operating at an accelerating voltage of 15 kV. A cryo-fracturing method was used to expose an internal surface without deforming the polymer during the fracturing process. The exposed surface was sputtered-coated with a thin layer of gold prior to examination.

3. RESULTS AND DISCUSSION

3.1. Rheological Behavior

Fig. 1 presents plots of shear stress against shear rate for the three sample sets at a measurement temperature of 30 °C. In all cases, the shear stress increases linearly with increasing shear rate, indicating that the systems behave in a Newtonian manner. These data also demonstrate that simple

addition of the as-received or calcined Si_3N_4 increases the viscosity of the epoxy resin by ~60 % in the absence of any thermal treatment of the mixture (*c.f.* 5U/100/0 and 5C/100/0 with 0U/100/0). Comparable nanoparticle effects on rheology have been reported elsewhere [36-38].

Iteratively heating the unfilled DGEBA at 100 °C and remeasuring its rheological behavior shows that this has no significant effect on the rheological properties of the system (see Fig. 1a); the data obtained from all specimens within the 0U/100/*t* sample set are equivalent. The same behavior can be seen for the samples filled with calcined Si_3N_4 (see Fig. 1c). Conversely, Fig. 1b shows that cyclically heating the DGEBA containing the as-received Si_3N_4 for 1 h periods results in a progressive increase in the viscosity of the mixture. This continues up to three cycles (total 3 h at 100 °C), after which, no appreciable further increases in viscosity occur. From these observations, we deduce the following:

(i) The lack of any increase in viscosity with increasing *t* within the 0U/100/*t* sample set indicates that neither repeated shearing nor heating at 100 °C results in sufficient chemical modification to the molecular structures present within the system – such as through homopolymerization – to affect the rheology of the unfilled DGEBA. Indeed, this aligns with previous studies [39-42] of similar epoxy resins, which have shown that homopolymerization is negligible at temperatures around 100 °C.

(ii) The lack of any variation in viscosity with increasing *t* within the 5C/100/*t* samples leads to three inferences. First, the imposed heating/shearing cycle does not cause detectable changes in the resin phase, which is expected based on the behavior of the unfilled samples (0U/100/*t*). Second, any changes in the state of dispersion of the nanoparticles as a result of the system being repeatedly sheared is not sufficient to modify its rheological characteristics [28]. Finally, the filler/resin mixture heating at 100 °C does not induce/accelerate any significant reactions between the epoxide groups of the DGEBA and any functional groups retained on the surface of the calcined Si_3N_4, which would modify the effective size of the nanoparticles and the nature of their interaction with the liquid matrix. Indeed, the imposed calcination process was chosen in order to favor the removal of hydroxyl and amine groups from the nanoparticle surfaces, effectively, to give a silica shell terminated with siloxane bridges around a Si_3N_4 core [32-34]. While it is conceivable this would not occur ideally, such that some hydroxyl groups might be retained, etherification reactions between epoxide and hydroxyl groups would not be favored at 100 °C [41,43]. In summary, the rheological invariance with *t* that is evident in Figures 1a and

1c is both internally consistent and consistent with expectations based upon complementary published work.

(iii) In addressing the origin of the progressive increase in viscosity with *t* within the uncalcined 5U/100/*t* sample set, we will consider the same three factors discussed above for the calcined 5C/100/*t* systems. First, an increase in viscosity may arise from changes in the chemistry of the fluid medium, but in view of the invariance in the viscosity of both the 0U/100/*t* and 5C/100/*t* systems, this seems unlikely. Second, an increase in viscosity may arise as a result of gross changes in the particle distribution state as a consequence of repeated shearing of the mixture. While this does not seem likely in view of the data obtained from 5C/100/*t* systems, a sample of 5U/100/1 was nevertheless rheologically characterized at 30 °C and then, without an intermediate heating step, directly subjected to repeat rheological characterization (Fig. 2). From Fig. 2, it is evident that the data obtained from the first and the second measurements are equivalent. In contrast, from Fig. 1b, it is evident that the data corresponding to 5U/100/1 and 5U/100/2 are different, whereby we conclude that the increase in viscosity exhibited by 5U/100/2 is not a consequence of the additional shearing experience by this system compared with 5U/100/1. Finally, chemical reactions may occur between the epoxy resin and functional groups on the surface of the uncalcined Si_3N_4. The surface chemistry of the as-received Si_3N_4 is characterized by the presence of both hydroxyl and amine groups [31-33], both of which may react with the terminal epoxide groups on the DER 332, resulting in a change in the surface structure and chemistry of the nanoparticles and an increase in their effective hydrodynamic radius, albeit that epoxide/hydroxyl groups reactions are not *per se* favored at 100 °C [41,43], as described above. Such a process would continue until all the accessible reactive functional groups are consumed or until further reactions are prevented by steric hindrance. From Fig. 1b, this occurs after ~3 h at 100 °C, such that heating for longer periods causes no further measurable viscosity increase. In contrast, the silica surface of calcined Si_3N_4 does not include the requisite amine functionality which is translated into an invariance of the viscosity of the 5C/100/*t* sample set on repeated heating at 100 °C, suggesting that the amine groups play a critical role in generating the observed response of the 5U/100/*t* systems.

To examine further the effect of repeatedly heating and shearing, additional rheological data were obtained at different measurement temperatures up to 50 °C. Fig. 3 contrasts data from the 5U/100/*t*

and 0U/100/*t* systems. The increase in viscosity with *t* is clear in all the data obtained from the former material system; in contrast the latter systems show no equivalent variation, which consolidates our previous conclusion. Also, it is evident that varying the rheological measurement temperature within the range shown does not affect the form of the observed behavior or the conclusions drawn. Assuming that reactions involving the particle surface amine groups and the epoxy groups are comparable to the reactively between the hardener's amine groups and the epoxy, then neither would occur to a great extent at temperatures well below the curing temperature, *i.e.* < 80 °C. As such, this invariance with measurement temperature is as expected.

(a)

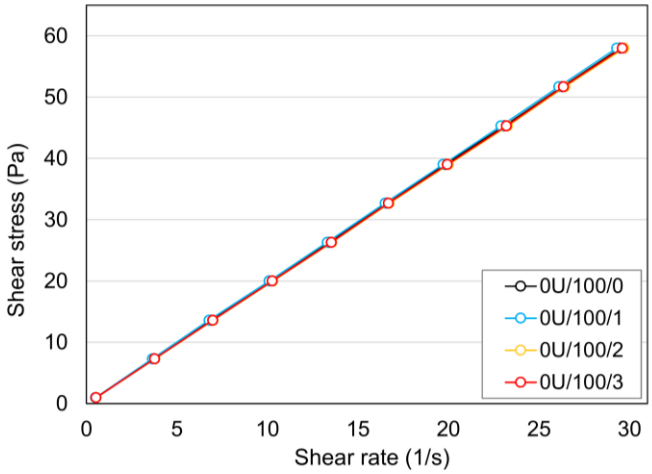

(b)

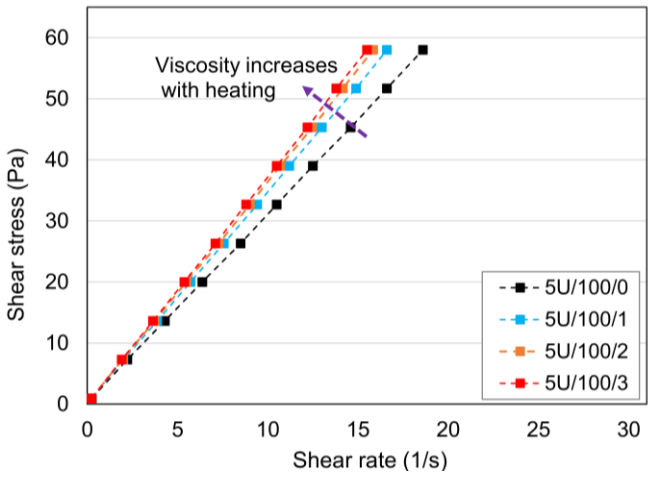

(c)

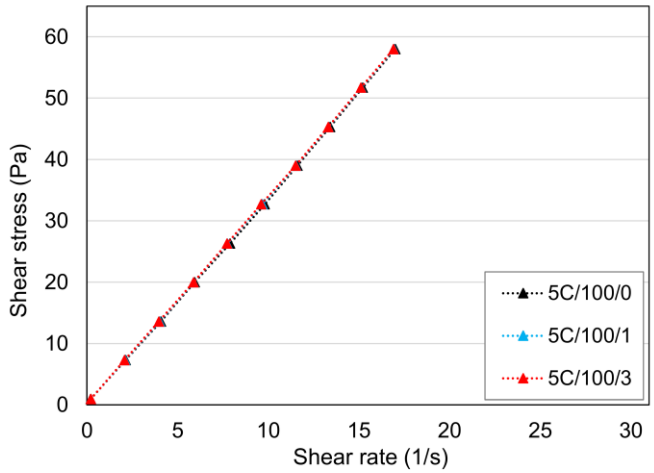

Fig. 1. Rheological data acquired at 30 °C from samples of: (a) 0U/100/*t*; (b) 5U/100/*t*; (c) 5C/100/*t*. The values of heating time, *t*, at 100 °C ranged from 0 to 3 h.

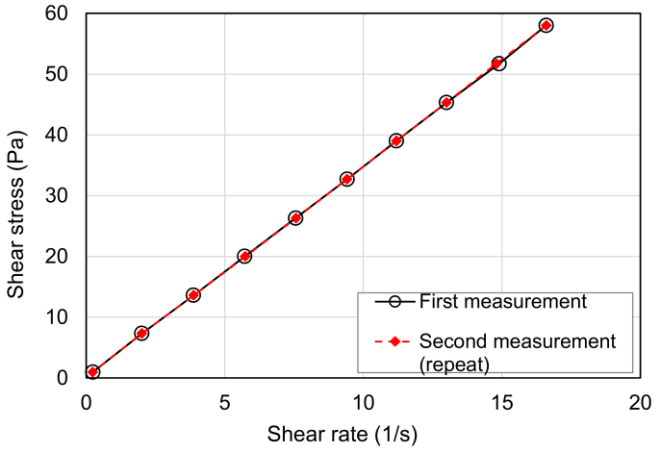

Fig. 2. Date obtained from measuring the rheological characteristics of sample 5U/100/1 twice at 30 °C.

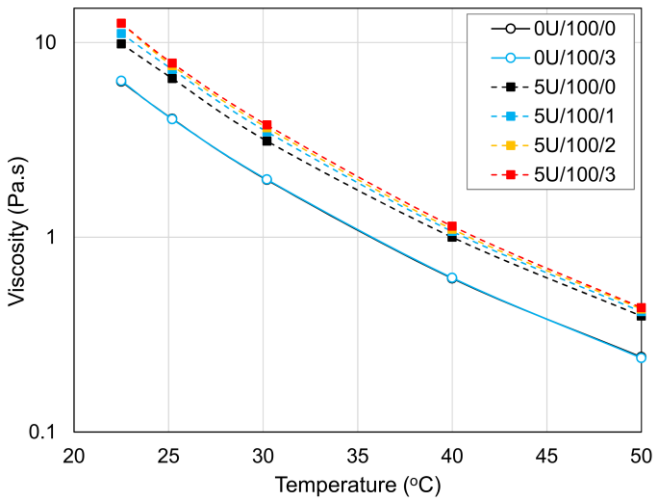

Fig. 3. Viscosity of unfilled and as-received Si_3N_4 filled epoxy samples at different measurement temperatures.

3.2. Particle Dispersion

To examine the impact of *t* on the resultant nanoparticle dispersion level within the 5U/100/*t* sample set, SEM images were obtained from a number of specimens; Fig. 4 shows representative images, obtained from 5U/100/0 and 5U/100/4. In neither system is there clear evidence of extensive (~10 μm) aggregates, a conclusion that aligns with previous studies of a range of different nanocomposites produced using the same grade of Si_3N_4 as used here [44]. While a precise interpretation of the detailed topography of these fracture surfaces is not easy, comparison of Fig. 4a and Fig. 4c shows that the latter exhibits a more uniform surface than the former, with the implication that the structure of 5U/100/0 is less homogeneous than 5U/100/4. Indeed, while the surface texture shown in Fig. 4b may be indicative of the presence of some loose agglomerations of primary particles in 5U/100/0, the equivalent image of sample 5U/100/4 suggests improved dispersion and smaller agglomerations. Thus, these images suggest that the sample with 4 h of isothermal heating has a better particle dispersion than the sample prepared without heating. Many studies [2,6,11,17] have showed that the dispersion of nanoparticles within a polymeric matrix depends on the interactions between the two components, with favorable interactions equating to a reduction in the Gibbs free energy of the system and, consequently, a better dispersion. Therefore, the better dispersion in the 5U/100/4 suggests stronger filler/matrix interactions that are brought with the heating step. In light of the above discussion, the improved particle dispersion of sample 5U/100/4 can be related to the longer

opportunity for the particles to react with the resin epoxide groups. Whereas many researchers have sought to improve nanoparticle dispersion by focusing on the surface chemistry of the particles and treating them with matrix-combatable functionalities, fewer studies have investigated the impact of the nanocomposite preparation method on the dispersion. The data presented above suggest that, even for a nanofiller that is inherently compatible with the chosen polymer matrix, the processing method may have a significant impact on the particle dispersion. Therefore, appropriately tailoring the fabrication method of nanocomposites is essential to achieve good nanoparticle dispersion in these systems.

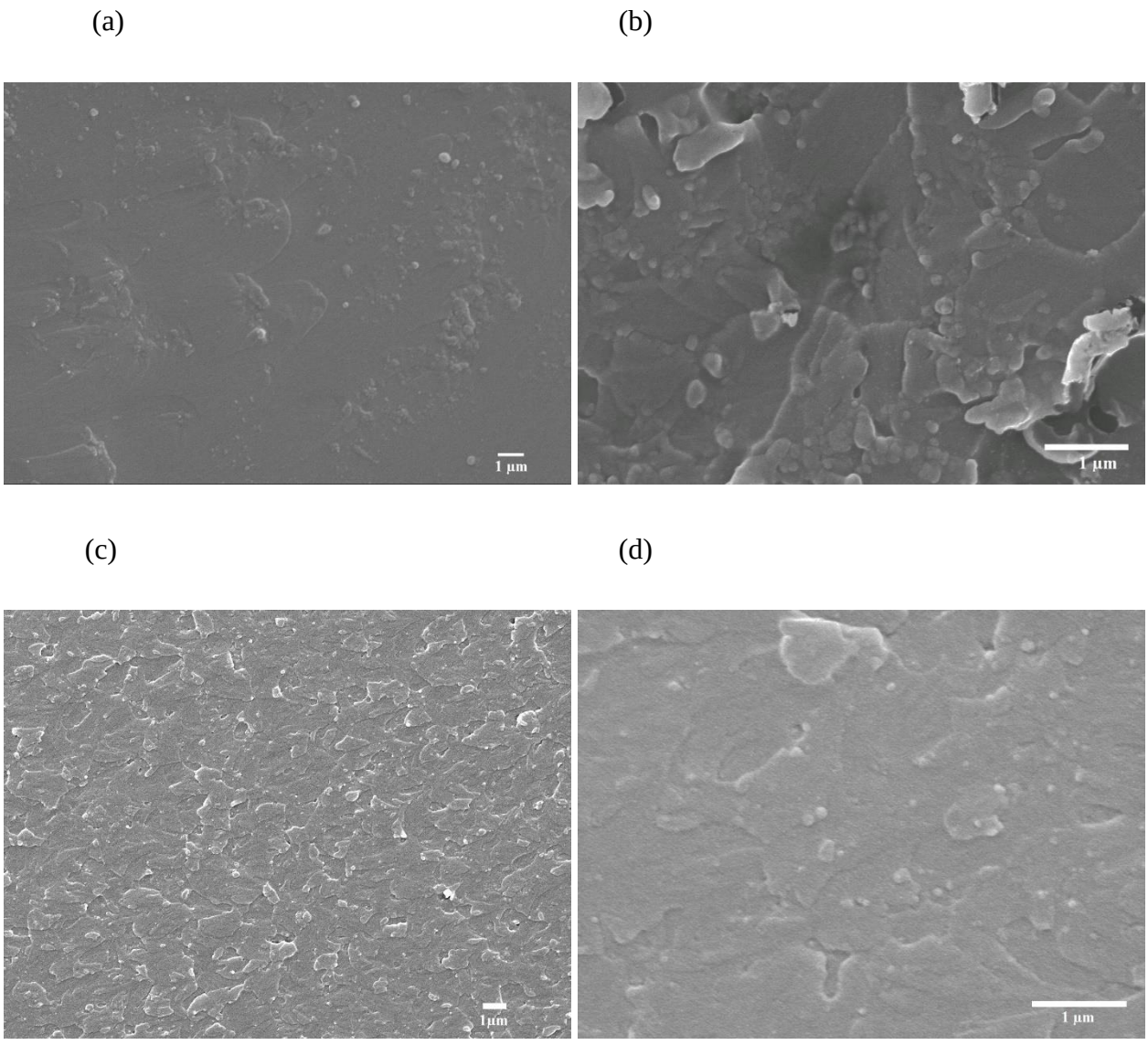

Fig. 4. Representative SEM images of fracture surfaces through: (a) and (b) 5U/100/0; (c)and (d) 5U/100/4.

3.3. Glass Transition Temperature

Fig. 5 shows the impact of heating time at 100 °C on the glass transition temperature of cured specimens from the three sample sets. For the unfilled and the calcined Si_3N_4 filled samples, T_g remains within measurement uncertainties, which indicates that the heating step does not affect T_g in these systems. This is consistent with the rheological behavior of these samples where the heating step, similarly, was shown not to lead to any measurable changes.

Conversely, in the 5U/100/*t* samples, T_g decreases markedly with increasing time of heating at 100 °C. Many studies of epoxy systems comparable to that considered here have concluded that T_g is strongly related to the crosslink density present in the network [40,45,46]. Consequently, we suggest that the reduction in T_g that is evident in the data acquired from the 5U/100/*t* systems in Fig. 5 is a result of a progressive reduction in crosslink density with increasing *t*, which may be explained as follows. Heating at 100 °C results in reactions between surface groups on the uncalcined Si_3N_4 nanoparticles and the terminal epoxide groups on the DER 332 resin. Such a process would result in a fraction of the epoxide groups from the DER 332 being consumed prior to instigation of matrix curing. Since the mass of hardener used throughout corresponds to the theoretically ideal stoichiometric ratio of DER 332 to Jeffamine D230, the proposed epoxy/Si_3N_4 reaction displaces the consequent matrix curing to a situation that equates to an effective excess of hardener; the number of amine groups present will then exceed the remnant number of epoxy groups, which leads to an amine (hardener)-rich network upon curing. Such excess in the amine groups will result in a reduction in the crosslinking density, since a fraction of the hardener molecules will remain unreacted [45]. Longer heating periods at 100 °C facilitate more reactions between the nanoparticles and the epoxy groups, which progressively reduces the number of remnant epoxy groups available to crosslink with the hardener amine groups and manifests itself as the observed reduction in T_g. This continues up to a heating duration of ~3 h, beyond which, further heating does not result in a significant reduction in T_g, with the implication that 3 h of heating at 100 °C leads to all the accessible reactive groups on the surface of the uncalcined Si_3N_4 being consumed. Such an interpretation is, again, entirely consistent with the rheological results described above.

The mechanism described above occurs as a result of thermal processing of the uncalcined Si_3N_4/epoxy mixture at 100 °C in the absence of any conventional hardener. Comparable reactions

between the uncalcined Si_3N_4 surface groups and the epoxy groups could also occur during the curing process (*i.e.* at 85 °C). This effect may be particularly important for the samples where the filler/resin mixture was not heated for a long duration before curing and thus most of the reactive nanoparticle surface groups will be potentially available to react with epoxy groups during the curing process. However, in this case, there will be a competition between such particle/resin reactions and the progressing crosslinking between the resin and the hardener. As curing progresses, the mobility of the resin molecules will reduce and, consequently, their reaction with the particle surface groups is expected to slow down and eventually stop. This mechanism can explain the relatively small reduction observed in the T_g of the sample without filler/resin heating before the curing process (Fig. 5). In this sample, a *fraction* of the reactive nanoparticle surface groups is expected to react with resin epoxide groups during the curing process, which yields a slightly amine-rich matrix that is characterized by a correspondingly reduced T_g.

To sum up, the reactions between nanoparticle surface groups and the epoxy groups changes the effective resin : hardener ratio of the matrix and the extent of this reaction and, consequently, the particle stoichiometric effect, critically depends on the material processing, in particular the temperature, of the filler/resin mixture before and during the curing process.

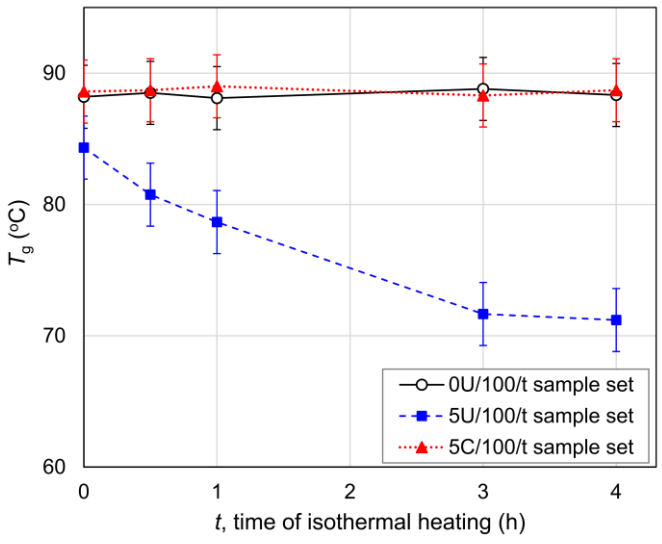

Fig. 5. The glass transition temperature of cured samples as a function of the duration of the heating step.

3.4. Dielectric Spectra

Dielectric data obtained from the 5U/100/*t* systems are contrasted with the unfilled, reference 0U/100/0 sample in Fig. 6: Figures 6a and 6b respectively shown the real (ε_r') and imaginary (ε_r'') parts of the relative permittivity. In Fig. 6b, a broad β relaxation process is evident in all four data sets, which peaks at 10^4 - 10^5 Hz. From these data, it is evident that the strength of this relaxation, $\Delta\varepsilon_r$, is greatest in the unfilled sample, 0U/100/0, and that this parameter progressively decreases within the 5U/100/*t* systems as *t* increases. In amine-cured epoxy systems, the β relaxation is generally attributed to motion of the hydroxyl ether groups that are produced during the crosslinking reaction between the epoxy and amine groups [47,48] and, therefore, the strength of this dielectric process should be related to the crosslinking density present in the system. As such, the progressive reduction in $\Delta\varepsilon_r$ with increasing *t* seen in Fig. 6b qualitatively mirrors the progressive reduction in T_g with increasing *t* evinced by Fig. 5; both factors stem from a reduction in crosslink density as a result of a progressive displacement of the effective matrix stoichiometry towards excess amines [45]. Another feature evident in the data presented in Fig. 6 is the gradual upturn in ε_r'' at low frequencies, which becomes more marked in the case of samples that had been subjected to heating at 100 °C. Previously, the DC conductivity of unfilled epoxy samples was reported to increase when residual amine groups were retained within the network[45], which in the dielectric spectrum would result in an increase in ε_r'' with decreasing frequency, particularly at low frequencies. As such, both the reduction in the strength of the β relaxation described above and the variation in ε_r'' at low frequencies are consistent with a progressive displacement of the curing reaction stoichiometry to an excess of amine groups as the total duration of filler/DGEBA heating is increased.

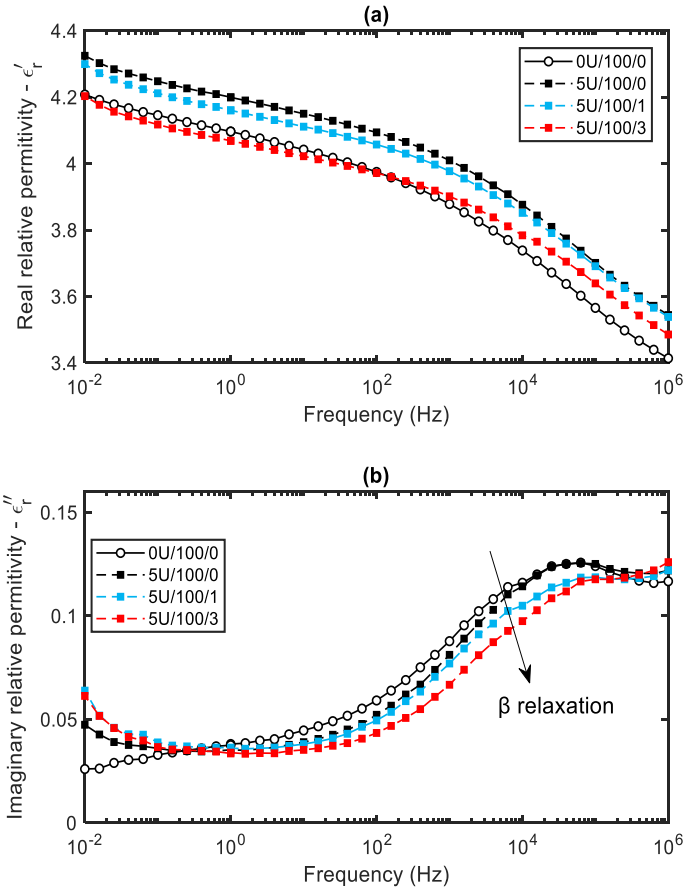

Fig. 6. Dielectric spectra obtained from 5U/100/*t* samples and the unfilled reference sample (0U/100/0).

While the dielectric data align well with the rheology and DSC data, all pointing towards reactions between the DER332 and functional groups on the surface of the uncalcined Si_3N_4, to test this assertion further, equivalent dielectric data to those presented in Fig. 6 were acquired from nanocomposites prepared using calcined Si_3N_4 which, from above, exhibit no increase in viscosity with increasing *t* (see Fig. 1c) and an invariant T_g (see Fig. 3). Fig. 7 shows the dielectric response of 5C/100/*t* samples, from which it is evident that these spectra do not appreciably vary as *t* increases. The slight variations in the spectra of 5C/100/0 and 5C/100/3 are within experimental uncertainties and all these spectra are comparable to the spectrum obtained from the unfilled, reference sample. Specifically, the invariance in the strength of the β relaxation indicates equivalent crosslinking across the 5C/100/*t* sample set; the absence of an increase in ε_r'' with decreasing frequency at low frequencies in any of the spectra indicates no appreciable variation in charge transport behavior and, therefore, no variation in the concentration of retained, unreacted amine groups [45]. In conclusion, the invariance

in the data presented in Fig. 7 supports the assertion derived from the rheological and glass transition temperature data that the calcination process removed most of the functional groups on the surface of Si_3N_4, such that the presence of calcined Si_3N_4 does not significantly influence matrix curing. The corollary of this being that the progressive variations seen in Fig. 6 support the notion that the presence of uncalcined Si_3N_4 *does* significantly influence matrix curing.

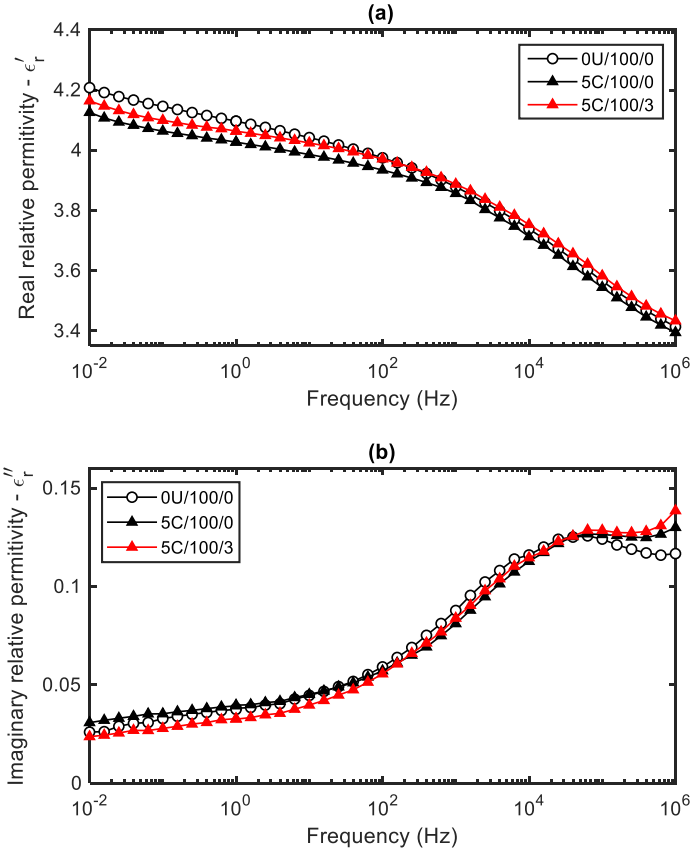

Fig. 7. Dielectric spectra obtained from 5C/100/*t* samples and the unfilled reference sample (0U/100/0).

We have previously reported on the influence of changes in stoichiometry on the molecular dynamics of the same epoxy/amine system reported here, as evinced by both the dielectric β relaxation and the glass transition [27]. These published data, together with those presented above, therefore, provide a means of determining the stoichiometric offset caused by the inclusion of 5 wt% of uncalcined Si_3N_4, from which, the associated number of additional reactive groups introduced into the system can be estimated. From Fig. 5, T_g of the 5U/100/4 system is characterized by a reduction in T_g of 17 °C;

assuming that this arises entirely as a result of an excess of primary amine groups within the system, this equates to an excess of hardener of 22% [27] or 3.5×10^{-4} mol of NH_2 per gram of material or 3.5×10^{-4} mol of NH_2 distributed over the surface of 50 mg of the Si_3N_4 nanopowder. From the relevant literature, it is evident that Si_3N_4 powders may be prepared in a number of ways. Cadete Santos Aires and Bertolini [49] indicated that grinding of bulk ceramics is commonly used commercially and that this generates crystalline powders of low specific surface area (<10 m^2/g). Kaskel and Schlichte [50] described a synthesis procedure that generated high surface area powders with specific surface areas ranging from 700 m^2/g to 1000 m^2/g depending on the imposed annealing temperature which, in their study, ranged from 600 °C to 1000 °C. Since the primary aim of the work of Kaskel and Schlichte concerned the catalytic activity of the final systems, no structural studies of the above systems were undertaken. Conversely, Kong et al. [51] described the production of silicon nitride-based aerogels based upon aggregated nanoparticles which, from the micrographs provided, appear to be ~100 nm in size and only began to show crystalline X-ray diffraction features when heated to at least 1500 °C. The amorphous Si_3N_4 produced at lower annealing temperatures were characterized by specific surface area values that ranged from 303 m^2/g to 638 m^2/g [51].

From the above account, it is evident that Si_3N_4 powders can be prepared in a number of ways and these result in products that differ greatly in terms of their internal structure and specific surface area. The system used in our study is described by the supplier as being amorphous and composed of particles less than 50 nm in size and, therefore, appears related to systems of the type described by Kong et al. [51]. Combining the above figure of 3.5×10^{-4} mol of NH_2 distributed over the surface of 50 mg required to generate the stoichiometric offset seen in Fig. 5 with a specific area value of 500 m^2/g (midrange, from the work of Kong et al. [51]; below the range reported by Kaskel and Schlichte [50]) leads to a surface density of amine groups of ~8 nm^{-2}. While we are unaware of any literature values for this quantity for amorphous Si_3N_4, the surface chemistry of silica has been well studied and, in that system, hydroxyl surface density values ranging from 2 nm^{-2} to 8 nm^{-2} have been reported [52-54]. Elsewhere, silica modified with low viscous poly(methylhydrosiloxane) and diethyl carbonate have been examined by nuclear magnetic resonance spectroscopy and shown to characterized by graft densities in the range 5 – 7 nm^{-2} [55]. While a value for amine surface density of ~8 nm^{-2} is not therefore incredible, the above estimation (a) assumes the presence of primary surface amines and (b) neglects the oxynitride nature of the Si_3N_4. In short, while the underlying mechanism is qualitatively credible and the inferred grafting density is consistent with that reported by Protsak et

al. [55], the precise local chemical interactions between amine, hydroxyl and epoxide groups that lead to the inferred degree of covalent grafting and/or non-covalent association require further investigation.

4. CONCLUSIONS

Filler/matrix interactions are widely cited as exerting an important impact on the properties of polymeric nanocomposites. However, the characterization of such local effects remains a challenge. In the work reported here, we have shown that filler/polymer interactions can affect the rheological characteristics of a nano-Si_3N_4 filled DGEBA-based epoxy resin system and, as such, that rheology may be used as an effective tool to detect such effects during nanocomposite preparation. Here, we associate the observed rheological changes with chemical reactions between amine groups on the surface of Si_3N_4 nanoparticles and epoxy groups within the DGEBA. These reactions increase the measured viscosity of the system, such that changing the temperature or duration of filler/resin mixing results in changes in the extent of filler/epoxy reactions. This proposition is supported by measurements of the glass transition temperature and dielectric spectra of such systems, which evince changes commensurate with an effective displacement of the curing reaction away from the ideal stoichiometry. That is, reactions between the nanofiller and the DGEBA during mixing at elevated temperature results in consumption of epoxide groups from the DGEBA, such that subsequent curing occurs under amine-rich conditions. This results in a reduction in the crosslinking density of the polymer matrix and, consequently, suppressed T_g values and a diminution of the strength of the dielectric β relaxation. Nominally small variations in the chosen material processing protocol (e.g. an increase in mixing temperature to reduce matrix viscosity with a view to improving nanoparticle dispersion) can inadvertently translate – for a system of fixed composition – to marked changes in ultimate macroscopic properties. We suggest that the significance of these results is twofold. First, the observation that different properties can be exhibited by the same material system when subjected to apparently equivalent processing may go some way to explaining the inconsistency in dielectric results reported in the literature for nominally equivalent nanofiller/polymer combinations. Second, our interpretation of the results reported here centers on the reaction of epoxide groups from the liquid medium with amine groups on the surface of the nanoparticles. This, we suggest, is limited by the number of available amine groups on the surface of the Si_3N_4 which, itself, may be controllable through thermal treatment – the calcined Si_3N_4 showed no increase in viscosity, suppression of T_g or

diminution in the strength of the dielectric β relaxation. Here, these reactions occurred in the liquid medium DGEBA, but many alternative epoxy-containing compounds may be used, with the implication that many different surface functionalities may be introduced in this way. The use of controlled calcination (to adjust the residual nanoparticle amine surface content) in concert with liquid phase processing (temperature, duration and choice of epoxide-containing liquid medium) may therefore provide a versatile means of adjusting the surface chemistry of inorganic nitride nanoparticles, in order to tailor their surface chemistry and thereby modify resulting nanocomposite properties. Furthermore, the chemical reactions involved appear rather more controllable than those involved when compounds such as trimethoxy silanes are used to tailor nanoparticle surfaces. Finally, in the case of systems such as those considered here, rheology provides a direct means of following the process without reliance on *post hoc* measurements.

CONFLICTS OF INTEREST

There are no conflicts of interest to declare.

DATA AVAILABILITY

The raw/processed data required to reproduce these findings cannot be shared at this time as

the data also form part of an ongoing study.

REFERENCES

[1] Wen Y, Yin Q, Jia H, Yin B, Zhang X, Liu P, et al. Tailoring rubber-filler interfacial interaction and multifunctional rubber nanocomposites by usage of graphene oxide with different oxidation degrees. *Compos. B Eng.* **2017**, *124*, 250-259.

[2] Kaldéus T, Träger A, Berglund LA, Malmström E, Re GL. Molecular Engineering of the Cellulose-Poly(Caprolactone) Bio-Nanocomposite Interface by Reactive Amphiphilic Copolymer Nanoparticles. *ACS Nano* **2019**, *13*, 6409-6420.

[3] Mohanty A, Srivastava VK. Dielectric Breakdown Performance of Alumina/Epoxy Resin Nanocomposites Under High Voltage Application. *Mater. Des.* **2013**, *47*, 711-716.

[4] Siddabattuni S, Schuman TP, Dogan F. Dielectric properties of polymer–particle nanocomposites influenced by electronic nature of filler surfaces. *ACS Appl. Mater. Interfaces* **2013**, *5*, 1917-1927.

[5] Roy M, Nelson JK, MacCrone RK, Schadler LS, Reed CW, Keefe R. Polymer Nanocomposite Dielectrics - the Role of the Interface. *IEEE Trans. Dielectr. Electr. Insul.* **2005**, *12*, 629-643.

[6] Šupová M, Martynková GS, Barabaszová K. Effect of Nanofillers Dispersion in Polymer Matrices: A Review. *Sci. Adv. Mater.* **2011**, *3*, 1-25.

[7] Starr FW, Douglas JF. Origin of Particle Clustering in a Simulated Polymer Nanocomposite and Its Impact on Rheology. *J. Chem. Phys.* **2003**, *119*, 1777-1788.

[8] Li Y, Krentz TM, Wang L, Benicewicz BC, Schadler LS. Ligand Engineering of Polymer Nanocomposites: From the Simple to the Complex. *ACS Appl. Mater. Interfaces* **2014**, 6, 6005–6021.

[9] Yang SQ, Wei BJ, Wang Q. Superior Dispersion Led Excellent Performance of Wood-Plastic Composites via Solid-State Shear Milling Process. *Compos. B Eng.* **2020**, *200*, 108347.

[10] Huang X, Liu F, Jiang P. Effect of Nanoparticle Surface Treatment on Morphology, Electrical and Water Treeing Behaviour of LLDPE Composites. *IEEE Trans. Dielectr. Electr. Insul.* **2010**, *17*, 1697-1704.

[11] Kim S-H, Rhee KY, Park S-J. Amine-Terminated Chain-Grafted Nanodiamond/Epoxy Nanocomposites as Interfacial Materials: Thermal Conductivity and Fracture Resistance. *Compos. B Eng.* **2020**, *192*, 107983.

[12] Whitby RLD. Chemical Control of Graphene Architecture: Tailoring Shape and Properties. *ACS Nano* **2014**, *8*, 9733–9754.

[13] Li YF, Zhang B, Pan XB. Preparation and characterization of PMMA− kaolinite intercalation composites. *Compos. Sci. Technol.* **2008**, *68*, 1954−1961.

[14] Miwa Y, Drews AR, Schlick S. Detection of the Direct Effect of Clay on Polymer Dynamics: The Case of Spin-Labeled Poly(methyl acrylate)/Clay Nanocomposites Studied by ESR, XRD, and DSC. Macromolecules **2006**, *39*, 3304-3311.

[15] Virtanen S, Krentz TM, Nelson JK, Schadler LS, Bell M, Benicewicz B, Hillborg H, Zhao S. Dielectric Breakdown Strength of Epoxy Bimodal-Polymer-Brush-Grafted Core Functionalized Silica Nanocomposites. *IEEE Trans. Dielectr. Electr. Insul.* **2014**, *21*, 563-570.

[16] Jia J, Sun X, Lin X, Shen X, Mai YW, Kim JK. Exceptional Electrical Conductivity and Fracture Resistance of 3D Interconnected Graphene Foam/Epoxy Composites. *ACS Nano* **2014**, *8*, 5774−5783.

[17] Cheng S, Xie SJ, Carrillo JMY, Carroll B, Martin H, Cao PF, Dadmun MD, Sumpter BG, Novikov VN, Schweizer KS, Sokolov AP. Big Effect of Small Nanoparticles: A Shift in Paradigm for Polymer Nanocomposites, *ACS Nano* **2017**, *11*, 752-759.

[18] Li K, Li Y, Lian Q, Cheng J, Zhang J. Influence of Cross-Linking Density on the Structure and Properties of the Interphase within Supported Ultrathin Epoxy Films. *J. Mater. Sci.* **2016**, *51*, 9019–9030.

[19] Tang Y, Ye L, Deng S, Yang C, Yuan W. Influences of Processing Methods and Chemical Treatments on Fracture Toughness of Halloysite-Epoxy Composites. *Mater. Des.* **2012**, *42*, 471-477.

[20] Zeng GB, Shi N, Hess M, Chen X, Cheng W, Fan TX, Niederberger M. A General Method of Fabricating Flexible SpinelType Oxide/Reduced Graphene Oxide Nanocomposite Aerogels as Advanced Anodes for Lithium-Ion Batteries. *ACS Nano* **2015**, *9*, 4227−4235.

[21] Yazdani H, Smith BE, Hatami K. Multi-Walled Carbon Nanotube-Filled Polyvinyl Chloride Composites: Influence of Processing Method on Dispersion Quality, Electrical Conductivity and Mechanical Properties. *Composites, Part A* **2016**, *82*, 65-77.

[22] Gupta ML, Sydlik SA, Schnorr JM, Woo DJ, Osswald S, Swager TM, Raghavan D. The Effect of Mixing Methods on the Dispersion of Carbon Nanotubes during the Solvent-Free Processing of Multiwalled Carbon Nanotube/Epoxy Composites. *J. Polym. Sci. B Polym. Phys.* **2013**, *51*, 410-420.

[23] Andritsch T, Kochetov R, Gebrekiros YT, Morshuis PHF, Smit JJ. Short Term DC Breakdown Strength in Epoxy Based BN Nano- and Microcomposites. *Proc. IEEE Int. Conf. Solid Dielectr., 10th* **2010**, 1-4.

[24] Qiang D, He M, Chen G, Andritsch T. Influence of Nano-SiO2 and BN on Space Charge and AC/DC Performance of Epoxy Nanocomposites. *IEEE Electr. Insul. Conf.,* **2015**, 492-495.

[25] Zammarano M, Maupin PH, Sung LP, Gilman JW, McCarthy ED, Kim YS, Fox DM. Revealing the Interface in Polymer Nanocomposites. *ACS Nano* **2011**, *5*, 3391−3399.

[26] Tian C, Feng Y, Chu G, Lu Y, Miao C, Ning N, et al. Interfacial Nanomechanical Properties and Chain Segment Dynamics of Fibrillar Silicate/Elastomer Nanocomposites. *Compos. B Eng.* **2020**, *193*, 108048.

[27] Alhabill FN, Ayoob R, Andritsch T, Vaughan AS. Influence of Filler/Matrix Interactions on Resin/Hardener Stoichiometry, Molecular Dynamics, and Particle Dispersion of Silicon Nitride/Epoxy Nanocomposites. *J. Mater. Sci.* **2018**, *53*, 4144-4158.

[28] Chu P, Zhang H, Chen F, Zhang Z. Rheological Behaviours of Nanosilica Suspensions with Different Dispersion Levels Prepared by the Bead Milling Technique. *Composites, Part A* **2016**, *81*, 34-40.

[29] Bar-Chaput S, Carrot C. Rheology as a tool for the analysis of the dispersion of carbon filler in polymers. *Rheol. Acta* **2006**, *45*, 339–347.

[30] Reading M, Vaughan AS. Dispersion and Rheology of Poly(ethylene oxide)/MMT Nanocomposites. *IEEE Conf. Electr. Insul. Dielectr. Phenom.* **2008**, 37-40.

[31] Tai YL, Qian JS, Miao JB, Xia R, Zhang YC, Yang ZG. Preparation and Characterization of Si3N4/SBR Nanocomposites with High Performance. *Mater. Des.* **2012**, *34*, 522−527.

[32] Stine R, Cole CL, Ainslie KM, Mulvaney SP, Whitman LJ. Formation of Primary Amines on Silicon Nitride Surfaces: A Direct, Plasma-Based Pathway to Functionalization. *Langmuir* **2007**, *23*, 4400−4404.

[33] Alhabill FN, Ayoob R, Andritsch T, Vaughan AS. Introducing Particle Interphase Model for Describing the Electrical Behaviour of Nanodielectrics. *Mater. Des.* **2018**, *158*, 62-73.

[34] Ni Z, Yang X, Yang X, He Q, Xu X, Xie H. Surface Modification of Ultrafine Silicon Nitride Powders by Calcination. *Int. J. Appl. Ceram. Technol.* **2019**, *16*, 1364– 1372.

[35] Alhabill FN, Andritsch T, Vaughan AS. On Water Absorption and Its Impact on the Dielectric Spectra of Epoxy Network with Different Stoichiometries. *Proc. IEEE Conf. on Electrical Insulation and Dielectric Phenomenon,* **2017**, 469-475.

[36] Geiser V, Leterrier Y, Manson JAE. Rheological Behaviour of Concentrated Hyperbranched Polymer/Silica Nanocomposite Suspensions. *Macromolecules* **2010**, *43*, 7705−7712.

[37] Matheson TN, Vaughan AS, Sutton SJ, Minigher A. Electrical Characteristics of Epoxy/nanoclay Nanodielectric Systems. *Proc. IEEE Int. Conf. Solid Dielectr., 7th* **2007**, 326-329.

[38] Haghtalab A, Marzban R. Viscoelastic Properties of Nanosilica-Filled Polypropylene in the Molten State: Effect of Particle Size. *Adv. Polym. Technol.* **2011**, *30*, 203-218.

[39] Bell J. Structure of A Typical Amine-Cured Epoxy Resin. *J. Polym. Sci. A-2 Polym. Phys.* **1970**, *8*, 417-436.

[40] Wang X, Gillham JK. Analysis of Crosslinking in Amine-Cured Epoxy Systems: The One-to-One Relationship Between Tg and Conversion. *J. Appl. Polym. Sci.* **1992**, *45*, 2127-2143.

[41] Turi E. Thermal Characterization of Polymeric Materials, *Academic Press*, 1981.

[42] Meyer F, Sanz G, Eceiza A, Mondragon I, Mijović J. The effect of stoichiometry and thermal history during cure on structure and properties of epoxy networks. *Polymer* **1995**, *36*, 1407-1414.

[43] Prolongo SG, Salazar A, Ureña A, Rodríguez J. Effect of Hydroxyl Content on the Morphology and Properties of Epoxy/Poly(Styrene-Co-Allylalcohol) Blends. *Polym. Eng. Sci.* **2007**, *47*, 1580-1588.

[44] Hosier IL, Praeger M, Vaughan AS, Swingler SG. The Effects of Hydration on the DC Breakdown Strength of Polyethylene Composites Employing Oxide and Nitride Fillers. *IEEE Trans. Dielectr. Electr. Insul.* **2017**, *24*, 3073-3082.

[45] Alhabill FN, Ayoob R, Andritsch T, Vaughan AS. Effect of Resin/Hardener Stoichiometry on Electrical Behaviour of Epoxy Networks. *IEEE Trans. Dielectr. Electr. Insul.* **2017**, *24*, 3739-3749.

[46] Morgan RJ, Kong FM, Walkup CM. Structure-Property Relations of Polyethertriamine-Cured Bisphenol-A-Diglycidyl Ether Epoxies. *Polymer* **1984**, *25*, 375-386.

[47] Jordan C, Galy J, Pascault JP. Measurement of the Extent of Reaction of an Epoxy–Cycloaliphatic Amine System and Influence of the Extent of Reaction on Its Dynamic and Static Mechanical Properties. *J. Appl. Polym. Sci.* **1992**, *46*, 859-871.

[48] Soles CL, Yee AF. A Discussion of the Molecular Mechanisms of Moisture Transport in Epoxy Resins. *J. Polym. Sci. B Polym. Phys.* **2000**, *38*, 792-802.

[49] Cadete Santos Aires FJ, Bertolini JC. On the Use of Silicon Nitride in Catalysis. *Top. Catal.* **2009**, *52*, 1492-1505.

[50] Kaskel S, Schlichte K. Porous Silicon Nitride as a Superbase Catalyst. *J. Catal*. **2001**, *201*, 270-274.

[51] Kong Y, Zhang J, Zhao Z, Jiang X, Shen X. Monolithic silicon nitride-based aerogels with large specific surface area and low thermal conductivity. *Ceram. Int.* **2019**, *45*, 16331–16337.

[52] McCrate JM, Ekerdt JG. Titration of free hydroxyl and strained siloxane sites on silicon dioxide with fluorescent probes. *Langmuir* **2013**, *29*, 11868-11875.

[53] Zhuravlev LT. The surface chemistry of amorphous silica. Zhuravlev model. *Colloids Surf. A Physicochem. Eng. Asp.* **2000**, *173*, 1-38.

[54] Madathingal RR, Wunder SL. Thermal degradation of poly(methyl methacrylate) on SiO_2 nanoparticles as a function of SiO_2 size and silanol density. *Thermochim. Acta* **2011**, *526*, 83-89.

[55] Protsak IS, Morozov YM, Dong W, Le Z, Zhang D, Henderson IM. A ^{29} Si, ^{1} H, and ^{13} C Solid-State NMR Study on the Surface Species of Various Depolymerized Organosiloxanes at Silica Surface. *Nanoscale Res. Lett.* **2019**, *14*(1), 160.